rf surface impedance of a two-band superconductor

Binping Xiao*

Collider-Accelerator Department, Brookhaven National Laboratory, Upton, New York 11973-5000, USA

C. E. Reece

Thomas Jefferson National Accelerator Facility, Newport News, Virginia 23606, USA

(Received 6 April 2018; published 6 May 2019)

In this paper, we extend the Mattis-Bardeen theory to obtain the surface impedance of a two-band superconductor, and apply it to magnesium diboride (MgB_2) for radiofrequency (rf) superconductivity applications. The numerical results for MgB_2 are in good agreement with the previously published experimental results. The surface impedance properties are clearly dominated by the smaller gap, significantly limiting utility in the 10-20 K regime that might otherwise have been attractive.

DOI: 10.1103/PhysRevAccelBeams.22.053101

I. INTRODUCTION

The recent activities of superconducting radiofrequency (SRF) accelerating cavities for the Linac Coherent Light Source II (LCLS-II) particle accelerator made from bulk niobium (Nb) materials are the state-of-art activities for high efficiency continuous wave accelerators for exploring frontier physics. The highest quality factor of single cell cavities was pushed to 7×10^{10} at 1.3 GHz and 2 K temperature [1], essentially fully exploiting the theoretical potential of niobium to accelerating field gradients of at least 20 MV/m [2]. Alternative superconducting materials with critical temperature and superheating critical field higher than those of Nb are of great interest as the next opportunity for continued technological progress. MgB_2 has been one of the candidate materials under investigation for possible future use in SRF applications since its discovery to be a superconductor by Nagamatsu *et al.* in 2001 [3]. MgB_2 is considered to be a conventional superconductor with a high critical temperature, T_c, of ~39–40 K [4]. It has two energy gaps, with a π-gap at 2.3 meV and a σ-gap at 7.1 meV [5–8], two corresponding coherence lengths between 1.6 and 5.0 nm and between 3.7 and 12.8 nm [4], and penetration depth between 85 and 203 nm [4]. At a temperature much lower than its critical temperature, the surface resistance is considered to be dominated by the π-gap, and could potentially be much lower than that of Nb considering that Nb's energy gap is 1.5 meV, and its critical temperature is 9.27 K. This feature also makes MgB_2 attractive for use in high-performance multilayer film coatings proposed by Gurevich [9].

Various tests have been made to measure the surface resistance and reactance of MgB_2 [10–13]. In reference [13], the authors used the surface impedance characterization (SIC) system [14] at Jefferson Lab (JLab) to test SRF properties of MgB_2 at 7.4 GHz, with temperature ranges from 2.2 K to critical temperature. This work was distinguished from the previous works by higher resolution [13].

Mattis and Bardeen (MB) [15], and Abrikosov, Gor'kov, and Khalatnikov (AGK) [16], independently derived the theory to calculate the surface impedance of single band BCS superconductors. These two theories have the same expression in the low field limit. Computer codes developed by J. Halbritter based on AGK and the one developed by J. P. Turneaure based on MB are routinely used to calculate the Nb surface impedance for SRF applications [17]. However, there is yet a lack of a treatment of the surface impedance of two-band superconductors based on MB or AGK. In this paper, we further extend the MB theory to obtain the surface impedance of MgB_2 and compare the simulated results with measured data [13].

II. RF SURFACE IMPEDANCE OF A TWO-BAND SUPERCONDUCTOR

Theoretical study of a two-band superconductor was initiated in 1959 [18]. The electrodynamic properties were extensively studied [19,20]. In this paper, we focus on the low field limit in which vortexes have not yet formed.

Following BCS theory [21], with temperature T close to 0, the probability of the state $(\boldsymbol{k}\uparrow, -\boldsymbol{k}\downarrow)$ being occupied by a pair of particles is h_k. With a finite T, single electrons start to appear. f_k is defined as the probability that state $\boldsymbol{k}\uparrow$ or $-\boldsymbol{k}\downarrow$, with Bloch energy relative to the Fermi sea of ε_k, being occupied, which follows the Fermi-Dirac distribution.

*binping@bnl.gov

We use subscripts d and s to represent different bands in the superconductor, energy gap A for band s, B for band d, and $E_{ks} = \sqrt{\varepsilon_{ks}{}^2 + A^2}$, $E_{kd} = \sqrt{\varepsilon_{kd}{}^2 + B^2}$.

In order to calculate the SRF BCS surface impedance, one may start with the matrix elements of a single-particle scattering operator as in Refs. [15,21]. The scattering between ks and $k's$, as well as the scattering between kd and $k'd$, should be the same as the case with single band gap. To calculate the effect brought by the scattering between kd and $k's$, and also between ks and $k'd$, we list the matrix elements in Table I. In these columns, h, h', f, f', E, E' are used to simplify the expressions of h_k, $h_{k'}$, f_k, $f_{k'}$, E_k, and $E_{k'}$, respectively. One may refer to Refs. [15,21] for more detail about this table.

While under rf field with angular frequency ω, the photon energy $\hbar(\omega - is)$ should be inserted into either the initial or the final state in Table I. Here a small positive parameter s, which will be set equal to zero in the final expression, has been introduced to obtain the real and imaginary part of surface impedance [15].

Based on the above analysis, the single-particle scattering operator, shown as Eq. (3.5) in Ref. [15] may be rewritten as,

$$I(\omega,R,T) = V_{ss}N_sN_sI_{ss}(\omega,R,T) + V_{dd}N_dN_dI_{dd}(\omega,R,T) + \frac{V_{sd}+V_{ds}}{2}N_sN_dI_{sd}(\omega,R,T) + \frac{V_{sd}+V_{ds}}{2}N_sN_dI_{ds}(\omega,R,T) \tag{1}$$

with

$$\begin{aligned}
I_{ss}(\omega,R,T) &= -\pi i\int_{A-\hbar\omega}^{\infty}[1-2f(E_{s2})][g(E_s,E_{s2},A,A)\cos(\alpha\varepsilon_{s2}) - i\sin(\alpha\varepsilon_{s2})]\mathrm{e}^{\mathrm{i}\alpha\varepsilon_s}dE_s\\
&\quad + \pi i\int_{A}^{\infty}[1-2f(E_s)][g(E_s,E_{s2},A,A)\cos(\alpha\varepsilon_s) + i\sin(\alpha\varepsilon_s)]\mathrm{e}^{-\mathrm{i}\alpha\varepsilon_{s2}}dE_s\\
I_{dd}(\omega,R,T) &= -\pi i\int_{B-\hbar\omega}^{\infty}[1-2f(E_{d2})]\times[g(E_d,E_{d2},B,B)\cos(\alpha\varepsilon_{d2}) - i\sin(\alpha\varepsilon_{d2})]\mathrm{e}^{\mathrm{i}\alpha\varepsilon_d}dE_d\\
&\quad + \pi i\int_{B}^{\infty}[1-2f(E_d)][g(E_d,E_{d2},B,B)\cos(\alpha\varepsilon_d) + i\sin(\alpha\varepsilon_d)]\mathrm{e}^{-\mathrm{i}\alpha\varepsilon_{d2}}dE_d\\
I_{sd}(\omega,R,T) &= -\pi i\int_{A-\hbar\omega}^{\infty}[1-2f(E_{s2})]\left[g(E_s,E_{s2},A,B)\frac{\varepsilon_s}{\varepsilon_s^*}\cos(\alpha\varepsilon_{s2}) - i\sin(\alpha\varepsilon_{s2})\right]\mathrm{e}^{\mathrm{i}\alpha\varepsilon_s^*}dE_s\\
&\quad + \pi i\int_{A}^{\infty}[1-2f(E_s)]\left[g(E_s,E_{s2},A,B)\frac{\varepsilon_{s2}}{\varepsilon_{s2}^*}\cos(\alpha\varepsilon_s) + i\sin(\alpha\varepsilon_s)\right]\mathrm{e}^{-\mathrm{i}\alpha\varepsilon_{s2}^*}dE_s\\
I_{ds}(\omega,R,T) &= -\pi i\int_{B-\hbar\omega}^{\infty}[1-2f(E_{d2})]\left[g(E_d,E_{d2},A,B)\frac{\varepsilon_d}{\varepsilon_d^*}\cos(\alpha\varepsilon_{d2}) - i\sin(\alpha\varepsilon_{d2})\right]e^{i\alpha\varepsilon_d^*}dE_d\\
&\quad + \pi i\int_{B}^{\infty}[1-2f(E_d)]\left[g(E_d,E_{d2},A,B)\frac{\varepsilon_{d2}}{\varepsilon_{d2}^*}\cos(\alpha\varepsilon_d) + i\sin(\alpha\varepsilon_d)\right]e^{-i\alpha\varepsilon_{d2}^*}dE_d
\end{aligned}$$

$$\begin{aligned}
&\text{and}\quad E_{s2} = E_s + \hbar\omega, \qquad E_{d2} = E_d + \hbar\omega \qquad \varepsilon_s^* = \sqrt{E_s{}^2 - B^2}, \qquad \varepsilon_{s2} = \sqrt{E_{s2}{}^2 - A^2},\\
&\varepsilon_{s2}^* = \sqrt{E_{s2}{}^2 - B^2}, \qquad \varepsilon_d^* = \sqrt{E_d{}^2 - A^2}, \qquad \varepsilon_{d2} = \sqrt{E_{d2}{}^2 - B^2}, \qquad \varepsilon_{d2}^* = \sqrt{E_{d2}{}^2 - A^2},\\
&g(E_1,E_2,\Delta_1,\Delta_2) = \frac{E_1E_2 + \Delta_1\Delta_2}{\varepsilon_1\varepsilon_2}, \qquad \alpha = \frac{R}{\hbar p_F}.
\end{aligned}$$

V_{ss}, V_{dd}, V_{sd}, and V_{ds} are the averaged interaction energies resulting from phonon emission and absorption by s-s, d-d, s-d, and d-s processes, minus the corresponding shielded Coulomb interaction terms [18]. N_s, N_d are the densities of states in the s and d bands near the Fermi level. The coefficient of I_{sd} takes into account the single particle scattering from s to d', as well as the scattering from d' to s. When $A = B$, (1) reduces to Eq. (3.5) in Ref. [15].

We use the SRF application of MgB_2 at 7.5 GHz range as an example. In this material the large energy gap is much bigger than the small energy gap. In this application $A - \hbar\omega > B$ holds in the temperature range the SRF application is interested in, i.e., from 0 K to 0.1 K below the critical temperature.

To obtain the surface impedance, we use the expressions in Ref. [22],

TABLE I. Matrix elements of single particle scattering operator (between ks and $k'd$).

Wave functions: Initial, ψ_i ks $k'd$	Final, ψ_f ks $k'd$	Ground (+) or excited (−) ks	$k'd$	Energy difference $W_i - W_f$	Probability of initial state	Matrix elements: $c_{k's\uparrow}{}^* c_{kd\uparrow}$ or $c_{-k's\downarrow}{}^* c_{kd\uparrow}$	$c_{-kd\downarrow}{}^* c_{-k's\downarrow}$ or $-c_{-kd\downarrow}{}^* c_{k's\uparrow}$
(a)		+	+	$E_s - E_{d'}$	$1/2s_s(1-s_{d'}-p_{d'})$	$[(1-h_s)(1-h_{d'})]^{1/2}$	$-(h_s h_{d'})^{1/2}$
X0 00	00 X0	−	−	$-E_s + E_{d'}$	$1/2s_s p_{d'}$	$(h_s h_{d'})^{1/2}$	$-[(1-h_s)(1-h_{d'})]^{1/2}$
X0 XX	XX X0	+	−	$E_s + E_{d'}$	$1/2s_s p_{d'}$	$-[(1-h_s)h_{d'}]^{1/2}$	$-[h_s(1-h_{d'})]^{1/2}$
		−	+	$-E_s - E_{d'}$	$1/2s_s(1-s_{d'}-p_{d'})$	$-[h_s(1-h_{d'})]^{1/2}$	$-[(1-h_s)h_{d'}]^{1/2}$
(b)		+	+	$-E_s + E_{d'}$	$1/2s_{d'}(1-s_s-p_s)$	$(h_s h_{d'})^{1/2}$	$-[(1-h_s)(1-h_{d'})]^{1/2}$
XX 0X	0X XX	−	−	$E_s - E_{d'}$	$1/2s_{d'} p_s$	$[(1-h_s)(1-h_{d'})]^{1/2}$	$-(h_s h_{d'})^{1/2}$
00 0X	0X 00	+	−	$-E_s - E_{d'}$	$1/2s_{d'}(1-s_s-p_s)$	$[h_s(1-h_{d'})]^{1/2}$	$[(1-h_s)h_{d'}]^{1/2}$
		−	+	$E_s + E_{d'}$	$1/2s_{d'} p_s$	$[(1-h_s)h_{d'}]^{1/2}$	$[h_s(1-h_{d'})]^{1/2}$
(c)		+	+	$E_s + E_{d'}$	$1/4s_s s_{d'}$	$[(1-h_s)h_{d'}]^{1/2}$	$[h_s(1-h_{d'})]^{1/2}$
X0 0X	00 XX	−	−	$-E_s - E_{d'}$	$1/4s_s s_{d'}$	$-[h_s(1-h_{d'})]^{1/2}$	$-[(1-h_s)h_{d'}]^{1/2}$
	XX 00	+	−	$E_s - E_{d'}$	$1/4s_s s_{d'}$	$[(1-h_s)(1-h_{d'})]^{1/2}$	$-(h_s h_{d'})^{1/2}$
		−	+	$-E_s - E_{d'}$	$1/4s_s s_{d'}$	$-(h_s h_{d'})^{1/2}$	$[(1-h_s)(1-h_{d'})]^{1/2}$
(d)		+	+	$-E_s - E_{d'}$	$(1-s_s-p_s)(1-s_{d'}-p_{d'})$	$[h_s(1-h_{d'})]^{1/2}$	$[(1-h_s)h_{d'}]^{1/2}$
XX 00	0X X0	−	−	$E_s + E_{d'}$	$p_s p_{d'}$	$-[(1-h_s)h_{d'}]^{1/2}$	$-[h_s(1-h_{d'})]^{1/2}$
00 XX		+	−	$-E_s + E_{d'}$	$(1-s_s-p_s)p_{d'}$	$-(h_s h_{d'})^{1/2}$	$[(1-h_s)(1-h_{d'})]^{1/2}$
		−	+	$E_s - E_{d'}$	$p_s(1-s_{d'}-p_{d'})$	$[(1-h_s)(1-h_{d'})]^{1/2}$	$-(h_s h_{d'})^{1/2}$

$$Z = i\pi\omega\mu_0 \left\{ \int_0^\infty ln[1 + K(p)/p^2] dp \right\}^{-1} \quad (2)$$

where

$$K(p) = \frac{-3}{4\pi\hbar v_F \lambda_L^2(0)} \int_0^\infty \int_{-1}^1 e^{ipRu} e^{-\frac{R}{l}} \times (1-u^2) I(\omega, R, T) du dR \quad (3)$$

with λ_L London penetration depth, and $K(p)$ the component that connects the Fourier components of current and vector potential [22].

One now obtains an analytical expression for the surface impedance by incorporating (1) into (3), then into (2).

A *Mathematica*™ program has been developed to calculate this integral. In calculations below we use the following parameters as a reference: $A_0 = 7.1$ meV, $B_0 = 2.3$ meV [8], $T_c = 39.5$ K [4], $l = 40$ nm, $\lambda_L = 100$ nm [4], Debye temperature $= 884$ K [23] and Fermi velocity $= 4.7 \times 10^5$ m/s [24], with outside conditions $T = 2$ K and frequency at 7.5 GHz. The interaction factors are $V_{sd} = 0.119$, $V_{ds} = 0.09$, $V_{ss} = 0.81$, $V_{dd} = 0.285$, [25] and $N_s = 1$, $N_d = 1.3$ [26,27].

Using the parameters above, the surface impedance of MgB_2 is calculated and compared with the experimental results in [13], with two samples having a 200 nm thick MgB_2 layer on sapphire (MgB_2-200-I and MgB_2-200-II), and one sample with 350 nm thick MgB_2 on sapphire (MgB_2-350). The surface resistance data and theory are shown in Fig. 1(a). Since the SIC system measures the changes of penetration depth (relative penetration depth), the measured and simulated results of relative penetration depth are shown in Fig. 1(b). The surface resistance data and theory agree above ~7 K. Below that temperature, the experimental surface resistance levels out and appears dominated by some residual resistance mechanism not included in the theory.

For comparison, the calculation results of the two-band analysis are compared with the results for single band superconductors. With all other parameters the same as the above, surface impedance at different energy gaps, at 7.1 meV (σ-gap), and 2.3 meV (π-gap) were calculated; results are shown in Fig. 1. As expected, the surface impedance of a two-band superconductor is greater than a single band superconductor with a σ-gap, and is smaller than that with a π-gap. The surface resistance is clearly dominated by the smaller π-gap [27,28]. The penetration depth can also be fitted by an effective gap [28], shown in Fig. 2 in Ref. [13] at 3.7 meV. In the dirty limit with l close to 0, calculation shows the contribution from interband scattering [sd and ds terms in Eq. (1)] is orders of magnitude lower than those from intra-band scattering [ss and dd terms in Eq. (1)]. This agrees with Ref. [27] and references therein.

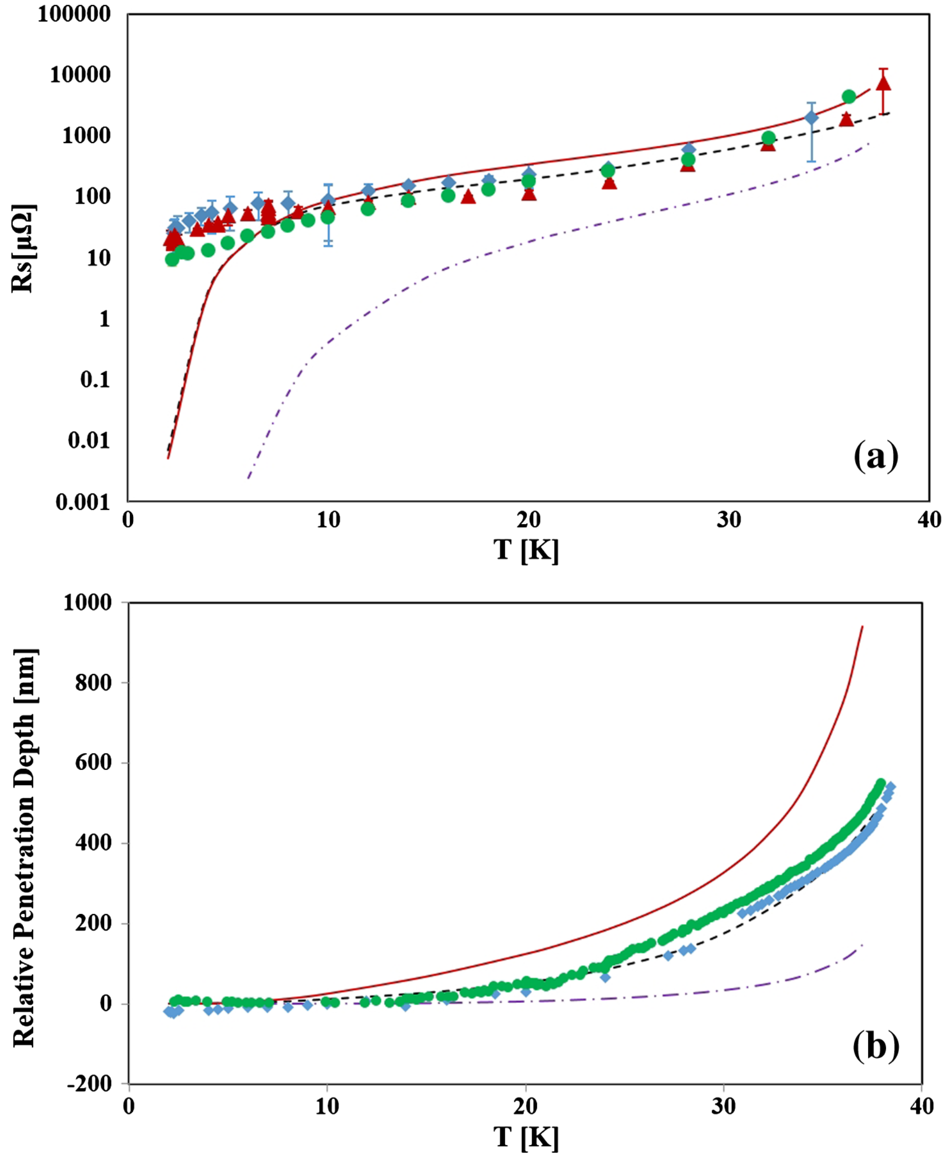

FIG. 1. (a) Surface resistance, and (b) relative penetration depth of MgB_2. Blue diamond MgB_2-200-I, red triangle MgB_2-200-II, green circle MgB_2-350, black dotted line is the two-gap analysis, red solid line is single π-gap calculation, and purple dash-dot line is single σ-gap calculation.

III. CONCLUSION AND DISCUSSION

With recent activities that are pushing the performance of Nb SRF cavities to their theoretical limits, the necessity of finding alternative materials for SRF application becomes more important. MgB_2, as the conventional superconductor with highest critical temperature, is a favorite candidate. By applying the theory of a two-band superconductor to the MB theory, we calculated the surface impedance of MgB_2. The results agree well with previously published experimental results.

Among all type I superconductors, MgB_2 has the highest critical temperature and thus is attractive for higher temperature SRF applications with corresponding lower cryogenic power demands, perhaps within range of closed-cycle cryocooling systems. In the sample measurement reported in Fig. 1, the residual resistance dominates at temperatures below 7 K. The mechanism(s) for these losses are yet unknown. Perhaps recent activities on Nb cavities [29,30] could be studied with MgB_2 thin films to further elucidate and suppress the residual resistance. Significant R&D is needed to make MgB_2 suitable for SRF applications at viable accelerating field gradients. First beneficial applications in accelerator systems could perhaps be in low-field regions that are at intermediate temperature, e.g., rf couplers, beamlines, or beamline bellows, which rely on bulk conduction cooling or use return liquid or gas helium from other SRF or superconducting magnet components.

ACKNOWLEDGMENTS

This work is supported by Brookhaven Science Associates, LLC under U.S. DOE Contract No. DE-AC02-98CH10886, and by Jefferson Science Associates, LLC under U.S. DOE Contract No. DE-AC05-06OR23177. The U.S. Government retains a nonexclusive, paid-up, irrevocable, world-wide license to publish or reproduce this manuscript for U.S. Government purposes.

[1] A. Grassellino, A. Romanenko, D. Sergatskov, O. Melnychuk, Y. Trenikhina, A. Crawford, A. Rowe, M. Wong, T. Khabiboulline, and F. Barkov, Nitrogen and argon doping of niobium for superconducting radio frequency cavities: A pathway to highly efficient accelerating structures, Supercond. Sci. Technol. **26**, 102001 (2013).

[2] B. P. Xiao, C. E. Reece, and M. J. Kelley, Superconducting surface impedance under radiofrequency field, Phys. C **490**, 26 (2013).

[3] J. Nagamatsu, N. Nakagawa, T. Muranaka, Y. Zenitani, and J. Akimitsu, Superconductivity at 39 K in magnesium diboride, Nature (London) **410**, 63 (2001).

[4] C. Buzea and T. Yamashita, Review of the superconducting properties of MgB_2, Supercond. Sci. Technol. **14**, R115 (2001).

[5] R. S. Gonnelli, D. Daghero, G. A. Ummarino, V. A. Stepanov, J. Jun, S. M. Kazakov, and J. Karpinski, Direct Evidence for Two-Band Superconductivity in MgB_2 Single Crystals from Directional Point-Contact Spectroscopy in Magnetic Fields, Phys. Rev. Lett. **89**, 247004 (2002).

[6] H. J. Choi, D. Roundy, H. Sun, M. L. Cohen, and S. G. Louie, The origin of the anomalous superconducting properties of MgB_2, Nature (London) **418**, 758 (2002).

[7] I. I. Mazin and V. P. Antropov, Electronic structure, electron–phonon coupling, and multiband effects in MgB_2, Phys. C **385**, 49 (2003).

[8] M. Iavarone, G. Karapetrov, A. E. Koshelev *et al.*, Two-Band Superconductivity in MgB_2, Phys. Rev. Lett. **89**, 187002 (2002).

[9] A. Gurevich, Enhancement of rf breakdown field of superconductors by multilayer coating, Appl. Phys. Lett. **88**, 012511 (2006).

[10] A. G. Zaitsev, R. Schneider, R. Hott *et al.*, Microwave properties of MgB_2 thin films prepared *in situ* by thermal evaporation combined with sputtering, J. Phys. Conf. Ser. **43**, 309 (2006).

[11] B. B. Jin, N. Klein, W. N. Kang, H.-J. Kim, E.-M. Choi, S.-I. Lee, T. Dahm, and K. Maki, Energy gap, penetration depth and surface resistance of MgB_2 thin films determined by microwave resonator measurements, Phys. Rev. B **66**, 104521 (2002).

[12] N. Klein, B. B. Jin, R. Wordenweber, P. Lahl, W. N. Kang, H.-J. Kim, E.-M. Choi, S.-I. Lee, T. Dahm, and K. Maki, Microwave properties of MgB_2 thin films, IEEE Trans. Appl. Supercond. **13**, 3253 (2003).

[13] B. P. Xiao, X. Zhao, J. Spradlin, C. E. Reece, M. J. Kelley, T. Tan, and X. X. Xi, Surface impedance measurements of single crystal MgB_2 films for radiofrequency superconductivity applications, Supercond. Sci. Technol. **25**, 095006 (2012).

[14] B. P. Xiao, C. E. Reece, H. L. Phillips, R. L. Geng, H. Wang, F. Marhauser, and M. J. Kelley, Radio frequency surface impedance characterization system for superconducting samples at 7.5 GHz, Rev. Sci. Instrum. **82**, 056104 (2011).

[15] D. C. Mattis and J. Bardeen, Theory of the anomalous skin effect in normal and superconducting metals, Phys. Rev. **111**, 412 (1958).

[16] A. Abrikosov, L. Gor'kov, and I. Khalatnikov, A superconductor in a high frequency field, Sov. Phys. JETP **35**, 182 (1959).

[17] J. P. Turneaure, J. Halbritter, and H. A. Schwettman, The surface impedance of superconductors and normal conductors: The Mattis-Bardeen theory, J. Supercond. **4**, 341 (1991).

[18] H. Suhl, B. T. Matthias, and L. R. Walker, Bardeen-Cooper-Schrieffer Theory of Superconductivity in the Case of Overlapping Bands, Phys. Rev. Lett. **3**, 552 (1959).

[19] E. Babaev, J. Carlström, M. Silaev *et al.*, Type-1.5 superconductivity in multicomponent systems, Phys. C **533**, 20 (2017).

[20] M. Silaev, T. Winyard, and E. Babaev, Non-London electrodynamics in a multiband London model: Anisotropy-induced nonlocalities and multiple magnetic field penetration lengths, Phys. Rev. B **97**, 174504 (2018).

[21] J. Bardeen, L. N. Cooper, and J. R. Schrieffer, Theory of superconductivity, Phys. Rev. **108**, 1175 (1957).

[22] P. B. Miller, Surface impedance of superconductors, Phys. Rev. **118**, 928 (1960).

[23] Z. F. Wei, G. C. Che, F. M. Wang, W. C. Wang, M. He, and X. L. Chen, Debye temperature of MgB_2, Mod. Phys. Lett. B **15**, 1109 (2001).

[24] A. Kohen and G. Deutscher, Symmetry and temperature dependence of the order parameter in MgB_2 from point contact measurements, Phys. Rev. B **64**, 060506 (2001).

[25] A. Gurevich, Enhancement of the upper critical field by nonmagnetic impurities in dirty two-gap superconductors, Phys. Rev. B **67**, 184515 (2003).

[26] K. D. Belashchenko, M. van Schilfgaarde, and V. P. Antropov, Coexistence of covalent and metallic bonding in the boron intercalation superconductor MgB_2, Phys. Rev. B **64**, 092503 (2001).

[27] B. B. Jin, T. Dahm, A. I. Gubin, E.-M. Choi, H. J. Kim, S.-I. Lee, W. N. Kang, and N. Klein, Anomalous Coherence Peak in the Microwave Conductivity of c-Axis Oriented MgB_2 Thin Films, Phys. Rev. Lett. **91**, 127006 (2003).

[28] G. Ghigo, D. Botta, A. Chiodoni, L. Gozzelino, R. Gerbaldo, F. Laviano, E. Mezzetti, E. Monticone, and C. Portesi, Effective gap at microwave frequencies in MgB_2 thin films with strong interband scattering, Phys. Rev. B **71**, 214522 (2005).

[29] A. Romanenko, A. Grassellino, A. C. Crawford, D. A. Sergatskov, and O. Melnychuk, Ultra-high quality factors in superconducting niobium cavities in ambient magnetic fields up to 190 mG, Appl. Phys. Lett. **105**, 234103 (2014).

[30] A. Romanenko, A. Grassellino, O. Melnychuk, and D. A. Sergatskov, Dependence of the residual surface resistance of superconducting radio frequency cavities on the cooling dynamics around Tc, J. Appl. Phys. **115**, 184903 (2014).